Dual-Wavelike Instability in Vortex Rings

JUN HUANG [1,2]
[1] Lappeenranta University of Technology
Department of Energy and Environmental
Engineering, 53810, Lappeenranta
Finland

KWOK TUNG CHAN [2]
[2]The Hong Kong Polytechnic University
Department of Mechanical Engineering
Hung Hom, Kowloon
Hong Kong, China

Abstract: A series of experimental observation are presented a dual-wavelike instability in vortex rings. The first one is presented at Reynolds number range between 600 and 1000 for circular vortex ring and the second one could be observed in radiant-symmetric vortex rings, azimuthal number $n \geq 2$, at least covers the Reynolds number from 275 to 1000. The azimuthal number of the first instability depends on the ratio η (of core radius to ring radius), while the azimuthal number of the second case accords with the shape of the orifice and the frequency of the second instability are also affected by the ratio η. The experimental results are compared with some theoretical prediction.

Key–Words: vortex ring, dual-wavelike, instability, azimuthal number, Reynolds number

1 Introduction

In the nearly thirty years, there has been a renewed interest into the oscillation in vortex ring. When Reynolds numbers smaller than 600, laminar vortex ring will form. If the Reynolds number is higher, about between 600 and 1000, the formed laminar vortex rings will transform to turbulence via an unstable azimuthal wave developing process. This azimuthal wave is the well-known instability of shortwave flexural perturbation with wavelength of the order of the vortex ring core radius. If Reynolds number is beyond this range, turbulent vortex ring will form from initial state [1]. Widnall & Sullivan [2] took some pictures to show this shortwave instability and also proved that a vortex ring in ideal fluid is always unstable theoretically. For a given vortex ring, only one unstable mode exists, depending on the size of the vortex core, the smaller ratio η, the larger azimuthal number n. The primary object of the present paper is to show another kind of wavelike phenomena in vortex rings. Superposing of this kind of waves could cause oscillations in different azimuthal number or oscillatory modes. The azimuthal number of this oscillation is independent of the ratio η but depend on the shape of the shape of the orifice, which is used to produce the vortex ring. However the ratio η maybe could affect the frequency of oscillation theoretical.

On the other hand, Stephen [3] compared Pochhammer-Chree theory with Timoshenko theory [4] of wave motion in cylindrical beam, showing a split character of the standing waves spectrum. Chan
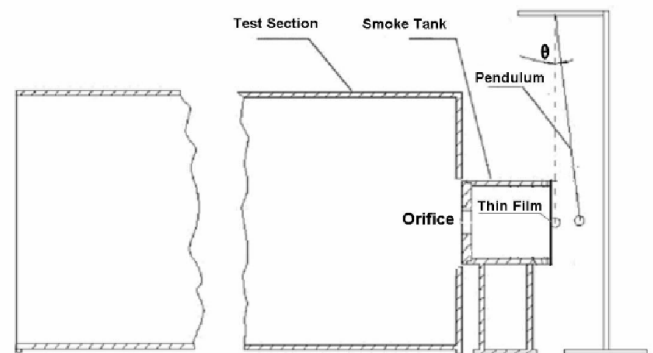
Figure 1: *Experimental apparatus*

et al. [5] detected this two-branch standing wave spectrum experimentally and named the two branches s_a-wave and s_b-wave. This dual-wave spectrum character is similar to that in vortex rings. Moreover, it could be found that the two processes are so analogous from the comparison of oscillation in vortex rings and that in solid rings.

2 Experimental Apparatus and Methodology

The experimental vortex rings generator could be divided into four parts: pendulum, smoke tank, orifice plates and test section, as shown in figure 1. In order to observe the motion of the vortex rings, the smoke tank was filled with incense smoke. The pendulum impacting the smoke tank would form vortex rings
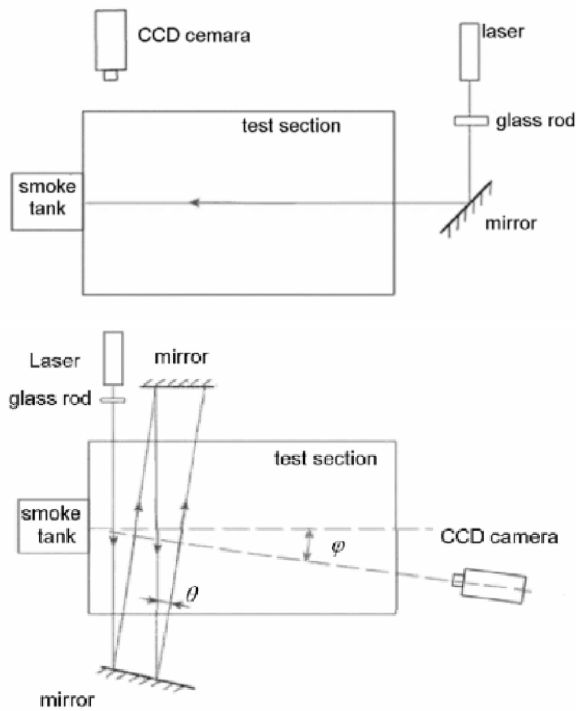
Figure 2: *upper: Optical geometry for side view and lower: Optical geometry for front view*

Figure 3: *Front view of an elliptical vortex ring when it passed the four fixed laser sheets*

from the orifices. In order to create the different initial boundary conditions, a series of orifices were employed, including one circular (D =20mm), two elliptical (28mm×14mm and 23mm×17mm), one triangular (side length 25mm) and one hexagonal orifice (side length 10mm). A small change of volume in the smoke tank due to impacting could prevent producing of turbulent vortex rings and therefore a thin plastic film was used, which makes the smoke tank looks like a drum. The test section was made of transparent synthetic resin, which prevented the outer flowing air affecting the experiments.

Schematics of the optical layout are shown in figure 2. Figure 2.a is used to take pictures of the front view and figure 2. b is for side view. Light from a 60mW, 628nm, He-Ne single-frequency continuous laser is focused on a glass rod and scattered to form a laser sheet. In figure 2.b the distances between the orifice and the four laser sheets are 20mm, 75mm, 95mm and 170mm respectively. The angle θ between inflection and incident laser sheets is about 7° and the CCD camera is inclined a small angle φ, which could increase the intensity of the light entering the camera. From the side view movie, the relationship between traveling time and distance for different initial velocity, or Reynolds number could be got. For noncircular orifices, the Reynolds number $Re = 4UR'/\nu$, where

R' is the equivalent radius and $R' = A/\chi$, where A is the area of the orifice and χ is wetted perimeter. For elliptical orifices, $\chi \approx \pi[1.5(a + b) - \sqrt{ab}]$. Therefore the equivalent radius of the 28mm×14mm elliptical orifice is 2.26mm and the equivalent radius of the 23mm×17mm is 2.56mm. In the front view geometry, a vortex ring could though four fixed laser sheets. Compared with the time- traveling distance relationship from side view, the initial velocities of the vortex rings in front view movie could be got.

3 Experimental Observation and Discuss

For vortex rings from the 28mm×14mm elliptical orifice, the periodic change of diameter was obvious. A series of front view pictures are shown in figure 3, which present the shapes of one vortex ring when it though the four laser sheets receptively. Another series of the relationships of diameter and distance are plotted in figure 4. The dots in this figure are collected from side view movies of seven vortex rings covering the range of Reynolds number about from 275 to 1000. Except the elliptical orifice for the vortex ring marked with black squares are rotated 90°, all the other vortex rings are produced from the same orifice at same location. It could be observed that the period of this change is independent of the traveling velocity, but due to the distance from the orifice. From this
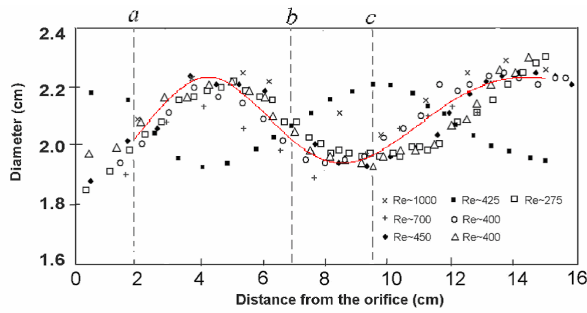
Figure 4: *The periodical changing of the diameters of seven vortex rings for the 28mm×14mm elliptical orifice. a, b and c are the locations for the pictures in figure 3. The distance for Figure 4.d is taken at 170mm, out of the range shown in this figure. The curve in this figure is used to fit the distribution of all the dots except the group marked by black squire by least square method.*
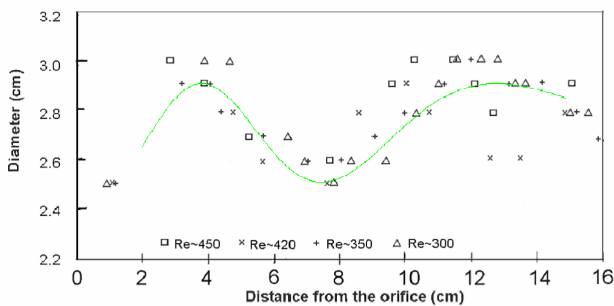
Figure 5: *The periodical changing of the diameters of vortex rings from the 23mm×17mm elliptical orifice. The curve in this figure is used to fit the distribution of all these dots by least square method.*

figure, the velocity of the vortex ring marked with $\triangle$ is very close to that marked with black squires, and therefore they could be thought as the data observed from two directions for a same initial condition. The two groups of dots are conjugated to each other. Combine the figures of front view and the data from side view, the change of diameters performs like an elliptical oscillation and it exits in a large range of Reynolds number, at least from 275 to 1000.

For vortex rings from the 23mm×17mm elliptical orifice, this oscillation also could be detected by the same methodology, although it is not as obviously as those from the 28mm×14mm elliptical orifice. Figure 5 is presented the change of diameter for these vortex rings. Because of using a common video

camera, the time between every neighboring dots in this figure is about 0.04 second (24 frame/second).

Two curves are used in figures 4 and 5 to describe the distribution of these dots. Both of the curves could be written as $D = D_o + D' \sin(kL + L_o)$, where k is the wave number. In fact, the size of the vortex rings would grow up a litter during the traveling process [6]. This process would decelerate the traveling velocity and affected the wave number k. Base on the hypothesis of k is a linear function of L, the mathematical expression for curves in figure 4 could be written as $D = 2.08 + 0.14 \sin[(1 - 0.02L)L + 2.4]$ and that in figure 5 could be written as $D = 2.7 + 0.2 \sin[(1 - 0.03L)L + 2.6]$. The algebraic expression of the two curves also could be written as $D = \mathbf{F}(L)$ in short, where the traveling distance L is a function of initial velocity and time. Thus the diameter could be written as a function of Re and t. Ignore the small change of frequency due to size, the diameter is depending on time only. The common form could be written as

$$D = D_o + D' \sin[\omega t + T] \qquad (1)$$

for a given Reynolds number, where ω is depending on Reynolds number. Figure 6 shows the linear relationship between Reynolds number and frequency f, which is proportional to ω, that $\omega = 2\pi f$.

In order to distinguish this kind of oscillation from the instability investigated by Widnall et al. [2],[7], figure 7 presents a couple of contrastive pictures. Both the two pictures are came from the 28mm×14mm elliptical orifice. The left one, figure 7.a was taken at a higher traveling velocity, $Re \approx 500$ and the figure 7.b was taken at a lower velocity, $Re \approx 300$. It is affirmed that the Widnall's instability only appears at higher Reynolds number, not only for circular vortex rings, but also for elliptical ones. It also could be known that the shortwave instability would appear at lower Reynolds number for elliptical vortex rings.

A similar oscillation also exits in the vortex rings from triangular orifices. A light geometry was used to detect this triangular oscillation, which is analogous that in figure 2, but a collimator was put between the laser and glass rod. This collimator could increase the diameter of the laser to illuminate a 3-D space, while not 2-D planes. Of course, this modification would weak the strength of the laser. Figure 8 shows three continuous frames from a movie by this light geometry. The time slots are 0.04s between every two neighboring flames. In figure 8.a, the vortex ring is ∇ shape and it evolves to $\triangle$ shape in figure 8.c gradually
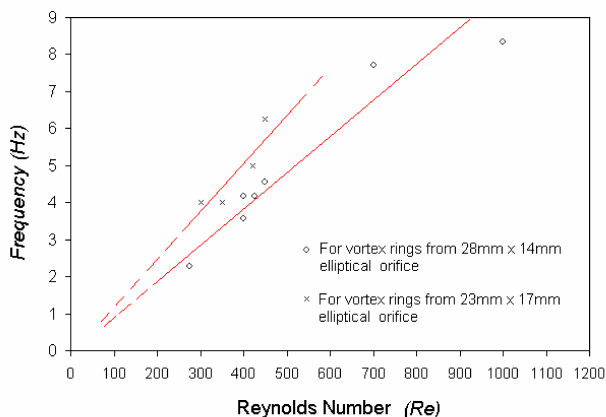
Figure 6: *Relationship between Reynolds numbers and frequencies. The frequencies equals the reciprocal of the first period in this figure.*

via figure 8.b. Experiments on polygonal vortex rings with more sides were also carried out, and some pictures also show the wavy pattern. However, it becomes difficulty to judge whether the pattern is caused by this oscillation or Widnall's shortwave instability.

The solution for the flexural wave motion in cylindrical beam is a family of curves, although only the lowest modes were found. Curves of the dispersion relation for waves in a straight vortex filament were given by Tsai et al. [8], which looks like that for cylindrical beam. It could be known that for a given wavelength, the ratio of wave frequency to the circulation is constant from Tsai et al's dispersion profile. On the other hand, Franenkel [9] gave a vortex ring traveling velocity expression including circulation,

$$U = \frac{\Gamma[\log \frac{8R}{a} - \frac{1}{4} + \eta^2(-\frac{3}{8}\log \frac{8}{\eta} + \frac{15}{32} + O(\eta^4 \log \frac{8}{\eta}))]}{4\pi R}$$

$$(2)$$

Base on the hypotheses for the oscillation in vortex rings is because of superposing of traveling waves in contrary direction, the wave frequency or the oscillation frequency should proportion to its traveling velocity U. This consequence agrees with the experimental results well.

Kopiev et al.[10] calculated the eigen-oscillations of vortex ring and found that the oscillation have a similar spectrum with that in vortex filament. A dimensionless frequency for Bessel modes was given,

$$\Theta = \frac{1}{2}m \pm [1 + O(\eta)] \qquad (3)$$
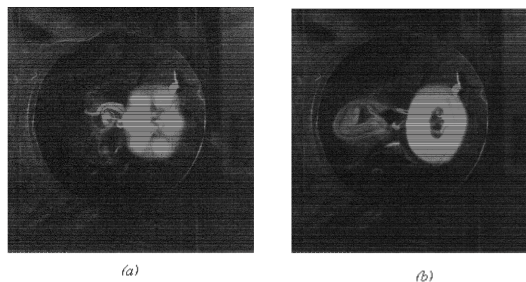
Figure 7: *Comparison of two elliptical vortex rings with different Reynolds number (a)$Re \approx 500$; (b)$Re \approx 300$.*
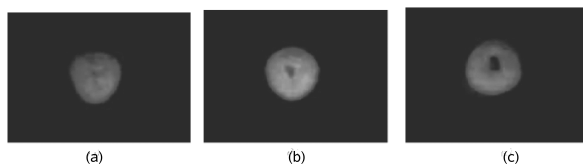
Figure 8: *Oscillation of triangular vortex ring, the time between every two flame is 0.04 second.*

where Θ is the ratio of oscillation frequency to rotation frequency of vortex ring core and m is wave shape number. When $m = 1$, it is a bending wave. A conclusion could be drawn from this equation that the dimensionless frequency is a constant for any flexural mode, and nevertheless the deduction of this equation is base on the Biot-Savart law. Combine the two equations, it could be got that the bigger equivalent radius R', the lower oscillation frequency for analogue shape vortex rings. However, the vortex rings from the 23mm×17mm elliptical orifice has a higher equivalent radius than that from the 28mm×14mm orifice, but with a higher frequency. Therefore, the difference of slopes in figure 6 could be thought as due to the effect of shape.

4   Summary and Conclusion

This visualization investigation has revealed the following characters concerning vortex rings instability: Firstly, there exists another wavy instability in vortex rings, which is different from the shortwave instability observed by Widnall et al. The wavelength of this instability is longer than that of shortwave instability. Secondly, this oscillatory instability covers a larger range of Reynolds number than shortwave instability. Thirdly, the shape of the orifice or its initial state determines the azimuthal wave number of this oscillation. Moreover, both the special period and the

temporal period of this oscillation would decrease if the elliptical oblatenesses increase. Furthermore, the aspect ratio of vortex rings is not depending on the elliptical oblatenesses of the orifice. Lastly, it was proven that special period is depending on the shape of the orifice only and the frequency of this oscillation is proportional to the traveling velocity and the circulation of the vortex ring experimentally and theoretically.

References:

[1] T. J. Maxworthy, The structure and stability of vortex ring, *Fluid Mech.* 51, 1972, pp. 15-32

[2] S. E. Midnall, J. P. Sullivan, On the stability of vortex ring *Proc. R. Soc. Lond. A* 332, 1973, pp. 335-353

[3] N. G. Stephen, The second frequency spectrum of Timshenko beam, *J. Sound Vib.* 80, 1982, pp. 578-582

[4] S. P. Timoshenko, On the transverse vibration of bars of uniform cross section, *Phil. Mag.* 43, 1922, pp. 125-131

[5] K. T. Chan, X. Q. Wang, R. M. C. So, S. R. Reid, Superposed standing waves in a Timoshenko beam *Proc. R. Soc. Lond. A*, 458, 2002, pp. 83-108

[6] K. Shariff, A. Leonard, Vortex rings, *Annu. Rev. Fluid Mech.* 24, 1992, pp. 235-279

[7] S. E. Widnall, C.-Y. Tsai, The instability of the thin Vortex ring of constant Vorticity, *Proc. R. Soc. Lond. A*, 287, 1977, pp. 273-305

[8] C.-Y. Tsai, S. E. Widnall, The stability of short waves on a straight vortex filament in a weak externally imposed strain field, *J. Fluid Mech.* 73, 1976, pp. 721-733

[9] L. E. Franenkel, Example of steady of vortex rings of small cross-section in ideal fluid, *J. Fluid Mech.* 51, 1972, pp. 119-131

[10] V.E. Kopiev, S. A. Chernyshev, Vortex ring eigen-oscillaitons as a source of sound, *J. Fluid Mech.* 341, 1997, pp. 19-57